

1  
2  
3  
4  
5  
6  
7  
8  
9  
10  
11  
12  
13  
14  
15  
16  
17  
18  
19  
20  
21  
22  
23  
24  
25  
26  
27  
28  
29  
30  
31  
32  
33  
34  
35  
36  
37  
38

## The $\alpha_{2A}$ -adrenergic receptor (*ADRA2A*) modulates susceptibility to Raynaud's syndrome

Anniina Tervi<sup>1\*</sup>, Markus Ramste<sup>2\*</sup>, Erik Abner<sup>3</sup>, Paul Cheng<sup>2</sup>, Jacqueline M. Lane<sup>4,5,6</sup>, Matthew Maher<sup>5</sup>, Vilma Lammi<sup>1</sup>, Satu Strausz<sup>1</sup>, Trieu Nguyen<sup>2</sup>, Mauro Lago Docampo<sup>8,14</sup>, Wenduo Gu<sup>2</sup>, *FinnGen*, *Estonian biobank research team*, Tõnu Esko<sup>3</sup>, Richa Saxena<sup>5,6,7</sup>, Aarno Palotie<sup>1,9,10,11</sup>, Samuli Ripatti<sup>1,5,12</sup>, Nasa Sinnott-Armstrong<sup>13</sup>, Mark Daly<sup>1,9,10,11</sup>, Marlene Rabinovitch<sup>14</sup>, Caroline A. Heckman<sup>1</sup>, Thomas Quertermous<sup>2</sup>, Samuel E. Jones<sup>1</sup>, Hanna M. Ollila<sup>1,5,6,7</sup>

1. Institute for Molecular Medicine Finland FIMM, Helsinki Institute of Life Science - HiLIFE, University of Helsinki, Helsinki, Finland
2. Division of Cardiovascular Medicine, Stanford University School of Medicine, Stanford, CA 94305
3. Institute of Genomics, University of Tartu, Tartu, Estonia
4. Division of Sleep and Circadian Disorders, Brigham and Women's Hospital and Harvard Medical School, Boston, MA, USA
5. Broad Institute of MIT and Harvard, Cambridge, MA, USA
6. Center for Genomic Medicine, Massachusetts General Hospital, Boston, MA, USA
7. Anesthesia, Critical Care, and Pain Medicine, Massachusetts General Hospital and Harvard Medical School, Boston, MA, USA
8. Stanford Cardiovascular Institute, Stanford University School of Medicine, CA.
9. Stanley Center for Psychiatric Research, Broad Institute of MIT and Harvard, Cambridge, MA, USA
10. Analytic and Translational Genetics Unit, Massachusetts General Hospital, Boston, MA, USA
11. Program in Medical and Population Genetics, Broad Institute of MIT and Harvard, Cambridge, MA, USA
12. Public Health, Faculty of Medicine, University of Helsinki, Helsinki, Finland
13. Herbold Computational Biology Program, Public Health Sciences Division, Fred Hutch, Seattle, WA, USA
14. Stanford Children's Health Betty Irene Moore Children's Heart Center, Department of Pediatrics, Stanford University School of Medicine, Stanford, CA, USA

\*Equal contribution

Correspondence: [anniina.tervi@helsinki.fi](mailto:anniina.tervi@helsinki.fi); [hanna.m.ollila@helsinki.fi](mailto:hanna.m.ollila@helsinki.fi)

## 39 Abstract

40

41 Raynaud's syndrome is a common dysautonomia where exposure to cold increases the  
42 vascular tone of distal arteries causing vasoconstriction and hypoxia, particularly in the  
43 extremities. Current treatment options are limited and unspecific. Biological  
44 mechanisms leading to the phenotype remain uncharacterized. Using genetic and  
45 electronic health record data from the UK Biobank, the Mass-General Brigham Biobank,  
46 the Estonian Biobank, and the FinnGen study, we identified 11,358 individuals with a  
47 diagnosis of Raynaud's syndrome and 1,106,871 population controls. We found eight  
48 loci including endothelial nitric oxide synthase (*NOS3*), HLA, and a notable association  
49 at the  $\alpha_{2A}$ -adrenergic receptor (*ADRA2A*) locus (rs7090046,  $P = 3.93 \times 10^{-47}$ ), implicating  
50 adrenergic signaling as a major risk factor with Raynaud's syndrome. We further  
51 investigate the role of the variants and *ADRA2A* expression in functional and  
52 physiological models. *In silico* follow-up analysis revealed an expression quantitative  
53 trait locus (eQTL) that co-localized and increased *ADRA2A* gene expression in a tissue-  
54 specific manner in the distal arteries. Staining with RNA scope further clarified the  
55 specificity of *ADRA2A* expression in small vessels. We show by CRISPR gene editing  
56 that the SNP region modifies *ADRA2A* gene expression in pulmonary artery smooth  
57 muscle cells. Finally, we performed a functional contraction assay on smooth muscle  
58 cells in cold conditions and showed lower contraction in *ADRA2A*-deficient and higher  
59 contraction in *ADRA2A*-overexpressing smooth muscle cells. Our results indicate that  
60 Raynaud's syndrome is related to vascular function mediated by adrenergic signaling  
61 through *ADRA2A*. Our study highlights the power of genome-wide association testing as  
62 a discovery tool for poorly understood clinical endpoints and further clarifies the role of

- 63 adrenergic signaling in Raynaud's syndrome by fine-mapping, using *in vitro* genomic
- 64 manipulations and functional validation in distal smooth muscle cell populations located
- 65 in arterioles

## 66 Main

67  
68 The autonomic nervous system controls physiological functions in the body that are not  
69 under direct voluntary control and are not typically consciously directed. The targets of  
70 the autonomic nervous system include body temperature, heart rate, respiration, bowel  
71 movements and digestion, sexual arousal, endocrine function, blood pressure regulation  
72 and vascular tone. However, when the autonomic nervous system malfunctions, it can  
73 lead to symptoms and diseases of dysautonomia, affecting many different functions of  
74 the autonomic nervous system including vascular tone and blood pressure as seen with  
75 Raynaud's syndrome (RS)<sup>1</sup>.

76 RS has a clear and specific disease manifestation, where the exposure to cold  
77 increases the vascular tone of distal arteries causing vasoconstriction, leading to  
78 cyanosis and hypoxia particularly in fingers and toes<sup>2</sup>. RS can be seen as an example  
79 of a disease with clear component of dysautonomia. Furthermore, RS is a common  
80 phenomenon, with an estimated prevalence of 3 to 5% in the global population<sup>3</sup>. RS  
81 rarely causes clinically debilitating symptoms, but RS is diagnosed with a single code in  
82 the international classification of diseases (ICD-10 I73.0<sup>4</sup>) making it possible to use  
83 electronic health records to find individuals with clinically significant RS and  
84 consequently understand RS disease manifestation, disease correlations and the  
85 underlying biological mechanisms.

86 Moreover, the comorbidities of RS include symptoms of pulmonary hypertension in a  
87 subset of patients, especially in patients with systemic sclerosis<sup>5-8</sup>. Consequently, RS  
88 can manifest as a comorbidity of diseases with substantial clinical significance, such as

89 systemic sclerosis, lupus erythematosus, myalgic encephalomyelitis/chronic fatigue  
90 syndrome, and most recently Long COVID<sup>9-11</sup>. Elucidating the disease mechanisms  
91 behind primary RS would potentially provide insight into diseases with dysautonomia<sup>12</sup>.  
92 Finally, RS has a relatively high hereditary component with estimated twin heritability  
93 between 54-65%<sup>13,14</sup>. This study is the first to examine genetic associations of RS  
94 across multiple cohorts and with functional validation in cellular models.

95

## 96 Results

97

### 98 $\alpha_{2A}$ -adrenergic receptor associates with Raynaud's syndrome

99 Using genetic and electronic health record data from FinnGen data freeze 10 (R10), the  
100 UK Biobank (UKB), the Estonian Biobank (EstBB), and the Mass General Brigham  
101 Biobank (MGB), we identified a total of 11,358 individuals with diagnosis of RS and  
102 1,106,871 controls. Demographic characteristics of in the study cohorts showed that the  
103 majority of RS patients were females (73.2 %), in agreement with earlier reports<sup>15,3</sup>, and  
104 mean disease diagnosis age was at 49.6 years (Suppl. Table 1).

105 Genome-wide association analysis of RS identified eight loci, which included a notable  
106 association at the  $\alpha_{2A}$ -adrenergic receptor (*ADRA2A*) locus, which was seen  
107 independently at genome-wide significant level ( $P \leq 5 \times 10^{-8}$ ) in all four cohorts and was  
108 further supported in the meta-analysis (rs7090046,  $P$  meta-analysis =  $3.93 \times 10^{-47}$ , beta  
109 [SE] = 0.22 [0.02], Figure 1, Table 1, Suppl. Figs. 1&2, Suppl. Tables 2,3,4).

110 In our meta-analysis, additional seven loci were genome-wide significant ( $P \leq 5 \times 10^{-8}$ ,  
111 Table 1). The variant rs7706161 is an intergenic variant closest to and downstream from  
112 *IRX1* (iroquois homeobox 1) gene. *IRX1* encodes for a homeobox gene involved in  
113 finger development in model organisms<sup>16</sup>. Furthermore, rs3130968 at chromosome 6 is  
114 located in the HLA region downstream from *HCG22* (HLA complex group 22) and  
115 upstream from the *HLA-C* and *HLA-B* genes. The same variant has also been  
116 associated with peripheral vascular disease<sup>17</sup>. Moreover, the lead genome-wide  
117 significant variant in chromosome 7, rs3918226, is an intron variant for *NOS3* (nitric  
118 oxide synthase 3/endothelial nitric oxide) 5' regulatory region. As endothelial nitric oxide  
119 signaling (eNOS) is a canonical mechanism in vasoconstriction and dilation<sup>18,19,20</sup>, our  
120 findings indicate a role for eNOS as part of vasoconstriction also in RS.

121 Variant rs7601684 in chromosome 2 is located upstream from *RAB6C*, a member of the  
122 RAS oncogene family. The other chromosome 2 variant, rs7559925, is an intron variant  
123 for the *ACVR2A* gene (activin A receptor type 2A) that encodes for a receptor related to  
124 activins, which are part of the TGF-beta (transforming growth factor-beta) family of  
125 proteins. Additionally, variant rs2092504 in chromosome 1, an intronic variant in  
126 transmembrane protein 51 (*TMEM51*), and variant rs191137443 in chromosome 4  
127 upstream from protocadherin 10 gene (*PCDH10*) were genome-wide significant in our  
128 meta-analysis. The association with rs7559925 was shown with immunological traits  
129 such as lymphocyte counts<sup>21</sup> whereas rs3918226 has been shown to be associated with  
130 high blood pressure<sup>22</sup>.

131 While many of these variants discovered in this GWAS are related to vascular tone,  
132 blood pressure or immune function, the *ADRA2A* locus stands out as a significant

133 association in all tested cohorts and biobanks, highlighting its importance in RS across  
134 multiple population cohorts. *ADRA2A* encodes for the  $\alpha_{2A}$ -adrenergic receptor, is  
135 targeted by  $\alpha$ -blockers, and has a downstream effect on lowering vascular tone and  
136 consequently blood pressure<sup>23-28</sup>.

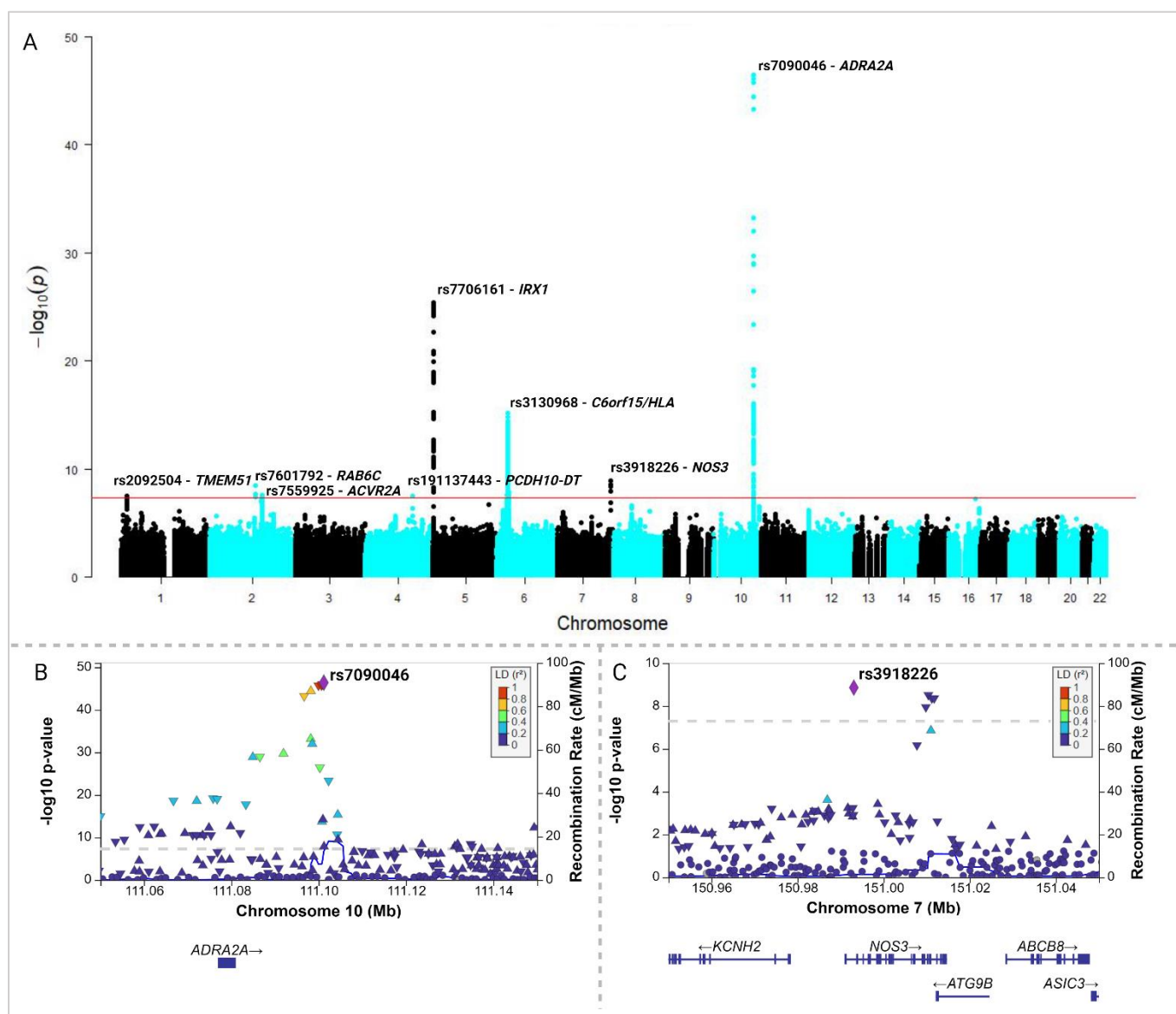


**Figure 1. Meta-analysis. A.** A Manhattan plot of RS meta-analysis combining UKB, FinnGen R10, MGB and EstBB. **B.** Locus zoom plots for regional association at the *ADRA2A* locus, lead variant rs7090046 and **C.** regional association at the *NOS3* locus, lead variant rs3918226. (Created with Biorender.com)

SNP	CHR	POS (b38)	Ref.	Alt.	Combined Alt.AF	P-value	Effect estimate (beta)	SE	Nearest gene
rs7090046	10	111101172	G	A	0.290	$3.93 \times 10^{-47}$	0.209	0.015	<i>ADRA2A</i>
rs7706161	5	4047779	A	G	0.725	$4.02 \times 10^{-26}$	-0.155	0.015	<i>IRX1</i>
rs3130968	6	31097294	T	C	0.147	$7.48 \times 10^{-16}$	0.157	0.019	<i>C6orf15/HLA</i>
rs3918226	7	150993088	T	C	0.076	$1.37 \times 10^{-09}$	0.148	0.024	<i>NOS3</i>
rs7559925	2	147883361	T	C	0.689	$2.88 \times 10^{-08}$	-0.079	0.014	<i>ACVR2A</i>
rs191137443	4	132501888	T	C	0.006	$2.99 \times 10^{-08}$	0.481	0.087	<i>PCDH10-DT</i>
rs2092504	1	15190856	T	C	0.415	$3.08 \times 10^{-08}$	-0.076	0.014	<i>TMEM51</i>
rs7601792	2	129324147	A	G	0.0076	$3.59 \times 10^{-08}$	0.590	0.107	<i>RAB6C</i>

**Table 1. RS meta-analysis lead variants** combining the UKB, FinnGen R10, MGB and EstBB data.

### 137 ***ADRA2A* RS risk variants increase *ADRA2A* expression**

138 To understand the functional consequences of the *ADRA2A* variants, we examined their  
139 association with gene expression across human tissues and tissue specificity. Using  
140 data from GTEx (<https://gtexportal.org/home/>), we observed that the lead variant  
141 (rs7090046) affected the expression of *ADRA2A* in a tissue-specific manner in the tibial  
142 arteries (rs7090046, eQTL  $P = 1.3 \times 10^{-13}$ , Figure 2) in contrast to coronary arteries ( $P =$   
143 0.16) or aorta ( $P = 0.65$ ). In addition, the lead variant for *ADRA2A* expression in GTEx  
144 in tibial arteries was rs1343449 ( $r^2$  in Europeans with rs7090046 = 0.98), which was  
145 also the lead variant in the MGB and among the five top variants in each cohort and the  
146 credible set (Figure 2, Suppl. Table 2). A formal co-localization analysis suggested a



147 shared signal between RS and *ADRA2A* expression in tibial arteries specifically  
 148 (posterior probability = 0.99, Figure 2, Suppl. Fig. 3, Suppl. Table 7). The risk allele  
 149 associated with higher RS risk associated with higher *ADRA2A* expression in  
 150 agreement with earlier role of adrenergic receptors regulating vascular wall  
 151 contraction<sup>29</sup>. Finally, we performed stratified LD score regression using ENCODE<sup>30</sup> to  
 152 elucidate overall relevance of different tissues across the body in RS. We discovered  
 153 the most significant associations with smooth muscle cell (SMC) types, further  
 154 suggesting that possible pathology is mediated by SMCs (Suppl. Table 5).

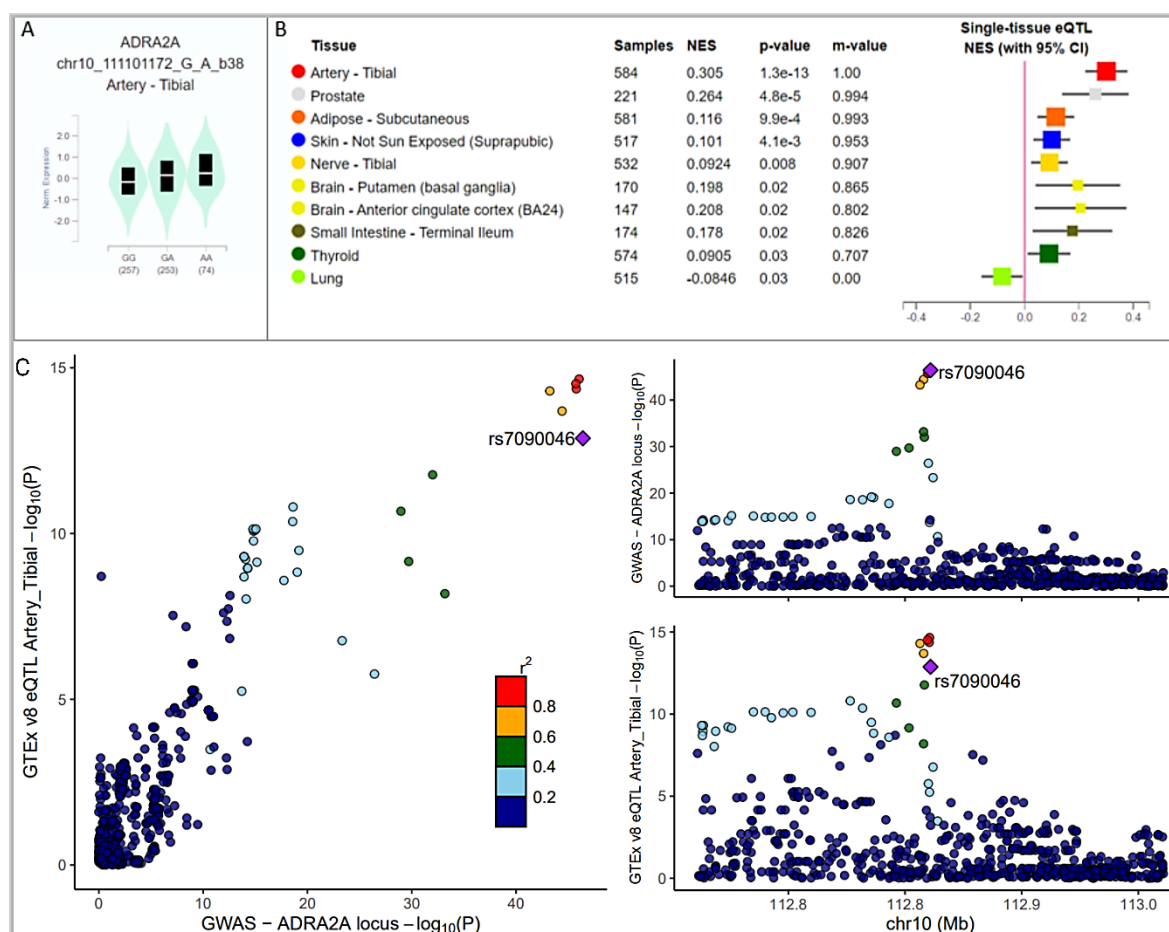


**Figure 2. *ADRA2A* expression.** **A.** Genotype-tissue expression for SNP rs7090046 in tibial arteries) and **B.** across tissues from GTEx (NES = normalized expression values, m-value = posterior probability,  $P \leq 0.05$ ). **C.** the RS association colocalizes with eQTL signal in tibial arteries. (created with Biorender.com)

155 ***ADRA2A* is specifically expressed in microvasculature**

156 Human arteries contain primarily fibroblasts, SMCs, pericytes (defined as cells found  
157 around microvasculature), and endothelial cells. As *ADRA2A* eQTL suggests that the  
158 variant affects expression in blood vessels in particular, we wanted to examine which  
159 cell types express *ADRA2A* in the vascular wall. First, single cell RNA sequencing  
160 (scRNAseq) data from human vascular tissue demonstrated that only a small cluster of  
161 cells expresses *ADRA2A* (Figure 3B). This cluster expressing *ADRA2A* is distinct from  
162 the medial smooth muscle cells (SMCs) that are the majority of the *MYH11*<sup>+</sup>, a classical  
163 marker for medial smooth muscle cells that are found in the vessel wall (Figure 3B &  
164 3D). Moreover, the cluster expressing *ADRA2A* contains cells that express mature SMC  
165 genes, and in addition co-express *NOTCH3* (Figure 3B & 3C)<sup>31,32</sup>. These findings  
166 suggest that only microvascular cells express *ADRA2A* and are likely a causal cell  
167 population for RS.

168 To further understand the role of the *ADRA2A* expressing cell population, we assessed  
169 the expression of *ADRA2A* in 14 different primary vascular smooth muscle cells.  
170 *ADRA2A* was found in only one line that was likely obtained from the pulmonary  
171 microvasculature but *ADRA2A* expression was otherwise not detected in any other  
172 vascular SMC lines derived from larger arteries including medium to large arteries  
173 (Figure 3F & 3G). This particular cell line also expresses other markers of the  
174 microvascular SMC population identified by scRNAseq, such as *NOTCH3* (Figure 3G).  
175 Thus, this microvascular SMC line was chosen for subsequent functional studies.

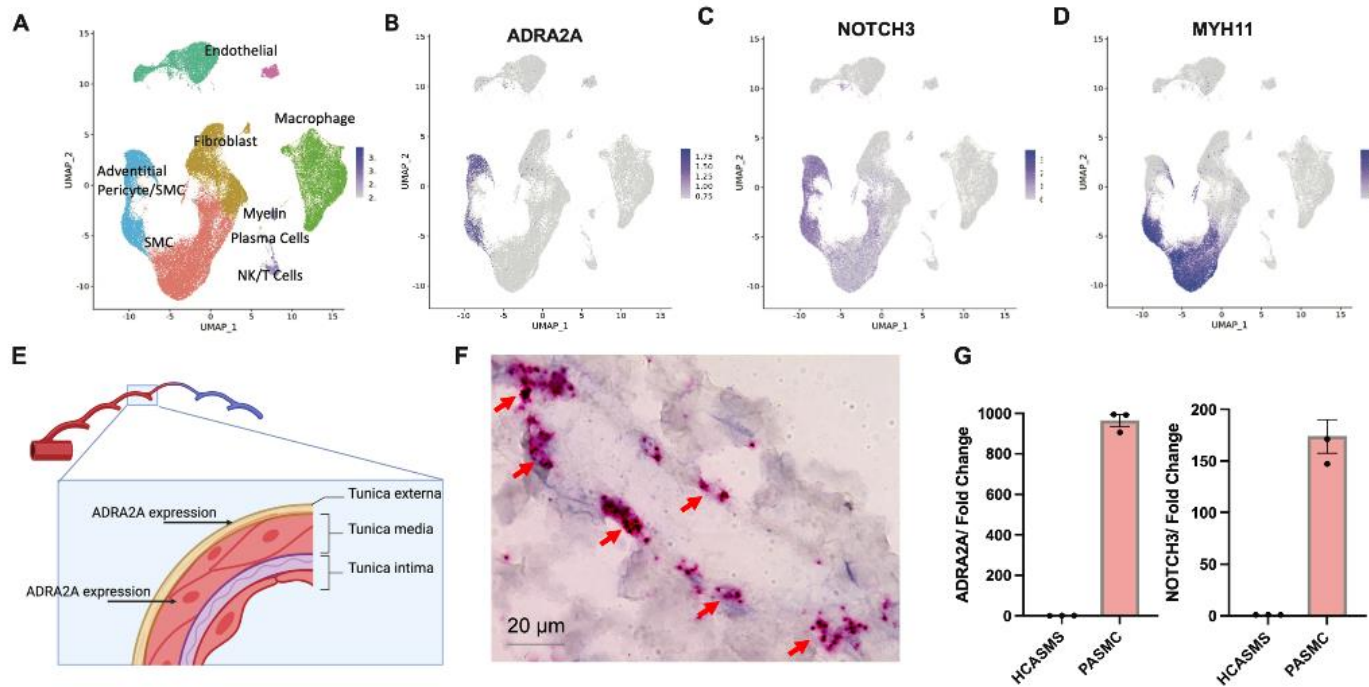


**Figure 3. *ADRA2A* expression is restricted to microvascular SMC.** UMAP plot of human artery scRNAseq from human vascular atlas indicating **A.** cell type identities of all clusters, **B.** *ADRA2A* expression, **C.** Co-expression of *NOTCH3* in the same cluster **D.** and *MYH11* expression. **E.** Schematic of vascular wall and *ADRA2A* expression. **F.** RNA Scope against *ADRA2A* in distal human coronary arteries **G.** RT-PCR quantification of *ADRA2A* and *NOTCH3* expression HCASMs and PASMCs.

176 ***ADRA2A* expression affects SMC contraction in temperature dependent fashion**

177 Next, we examined how *ADRA2A* expression alters SMC contractility in conditions  
178 mimicking RS and environmental cold stress. Earlier studies in temperature-dependent  
179 vascular contraction have supported the role of the adrenergic system but have focused  
180 nearly solely on the role of *ADRA2C* and its temperature-dependent activation<sup>26,33,34</sup>.  
181 These earlier studies and our findings raise an interesting question: Does *ADRA2A*  
182 directly affect vascular contraction? To test this, we used a collagen-based SMC  
183 contraction assay in *ADRA2A* over-expressing or silenced cells. We discovered that in  
184 cold conditions (+28°C), silenced siRNA-*ADRA2A* treated pulmonary artery SMCs  
185 (PASMCS) contracted significantly less (Figure 4A). However, *ADRA2C* silencing did  
186 not attenuate cold induced contraction in a similar manner to *ADRA2A* (Figure 4A). In  
187 warm conditions, both *ADRA2A* and *ADRA2C* silenced SMCs contracted similarly  
188 (Figure 4B). Consequently, upon lentiviral overexpression of *ADRA2A*, we observed  
189 that the PASMCS contracted significantly more (Figure 4C, D) overall suggesting that  
190 *ADRA2A* was affecting contraction in a dose dependent fashion and was responsible for  
191 cold induced contraction.

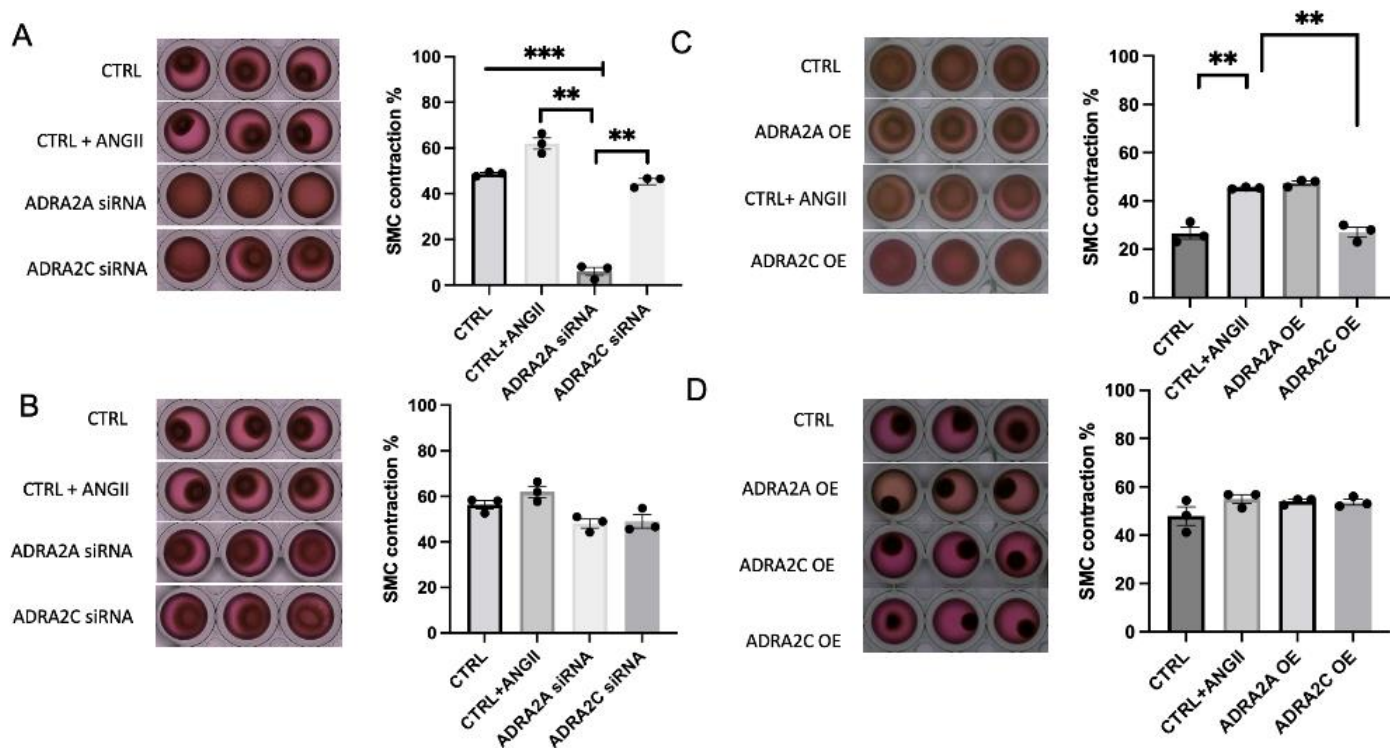


**Figure 4. ADRA2A expression affects SMC contraction upon cold stimulus (+28°C).** A. *ADRA2A* and *ADRA2C* silencing in cold exposure B. *ADRA2A* and *ADRA2C* silencing and in ambient conditions C. *ADRA2A* and *ADRA2C* overexpression in cold exposure D. *ADRA2A* and *ADRA2C* overexpression in ambient conditions. Mean +/- SEM, \*\*\* $P < 0.0005$ , \*\* $P < 0.005$  & \* $P < 0.05$ .

192 **CRISPR interference targeting rs7090046 supports *ADRA2A*'s role as a causal**  
193 **gene for RS**

194 We then used this cell line to study *ADRA2A* gene causality in RS. To elucidate  
195 mechanistic importance of the *ADRA2A* rs7090046 locus, we designed five CRISPR  
196 guides targeting the lead SNP variant rs7090046 and used the CRISPRi-Cas9  
197 machinery to interfere signaling from this variant region. We observed a significant  
198 decrease in *ADRA2A* gene expression 5 days after the lentiviral treatment on the  
199 PSMCs suggesting that the region is needed for controlling *ADRA2A* expression  
200 (Figure 5).

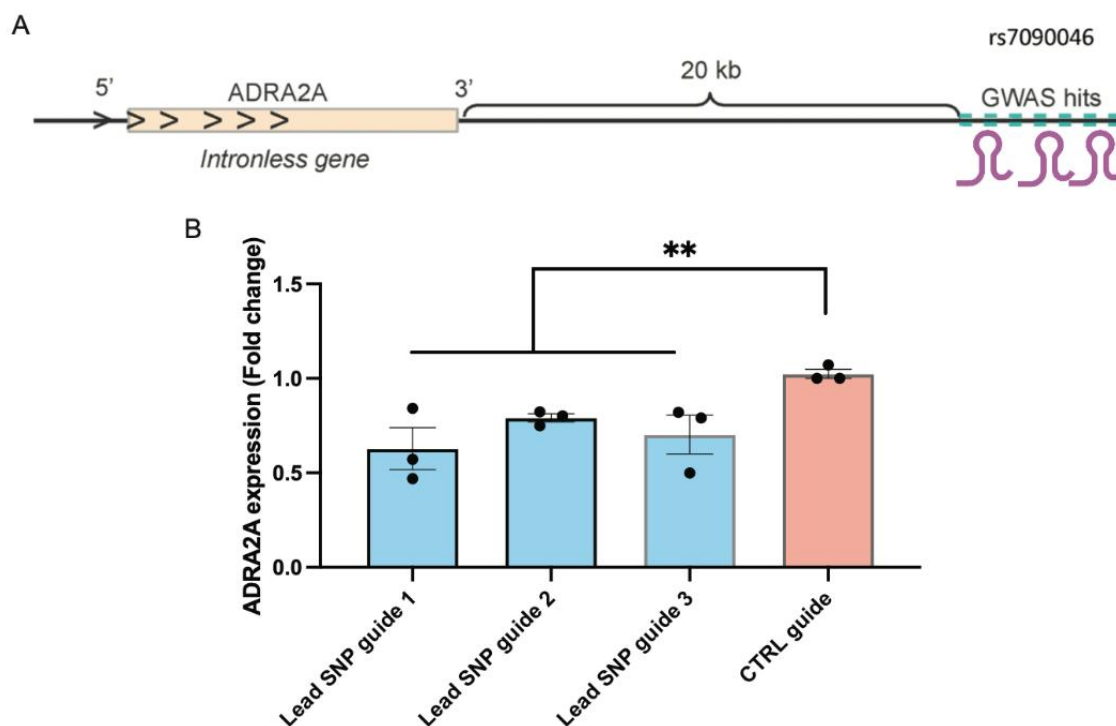


**Figure 5. CRISPR interference against rs7090046 supports causal role of *ADRA2A*.** A. Schematic of the CRISPR interference experiment. B. RT-PCR quantification of *ADRA2A* expression in rs7090046 guide targeted cells vs CTRL. Mean +/- SEM, \*\*\*P<0.0005, \*\*P<0.005 & \*P<0.05.

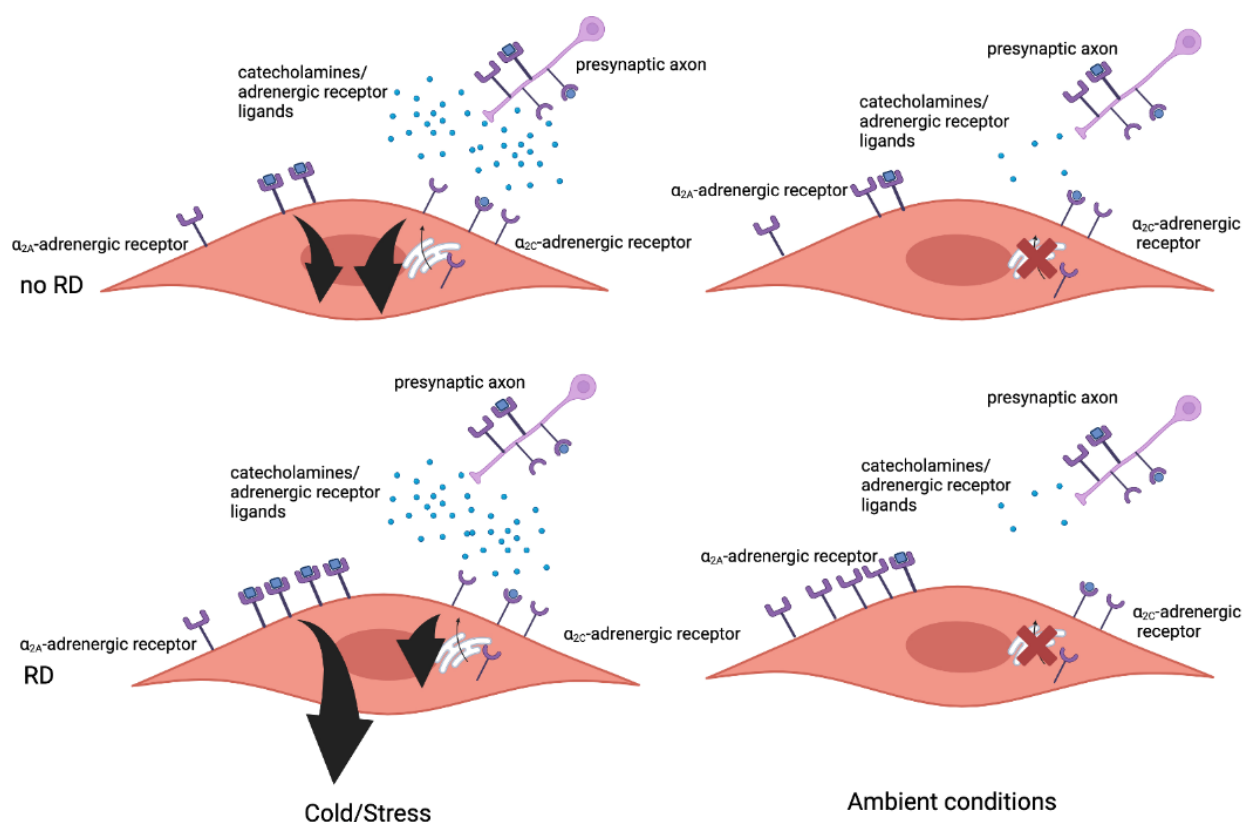


**Figure 6. Schematic of the proposed RS –associated pathomechanism. We propose a possible mechanism based on our observations from genetic and contraction assays.** In this hypothesized model, the pathomechanism of RS is dependent on *ADRA2A* expression. In normal physiological conditions, it is well established that cold or stress both induce secretion of the ligands that bind the adrenergic receptors. Consequently, these ligands such as epinephrine and norepinephrine activate the adrenergic system. In RS patients, the expression of *ADRA2A* gene encoding  $\alpha$ 2A-adrenergic receptor is higher and similarly the amount of  $\alpha$ 2A-adrenergic receptor available for ligand binding on microvascular SMCs. Increase in SMC *ADRA2A* expression sensitizes the postsynaptic system that aggravates adrenergic effects of SMC contraction. In conditions such as cold and stress where more ligand is released the contraction is further accentuated. Black arrows representing adrenergic downstream signaling strength.

## 201 Discussion

202

203 We performed a meta-analysis of RS across four cohorts and identified genome-wide  
204 significant associations with RS at *ADRA2A*, *HLA*, *NOS3*, *RAB6C*, *ACVR2A*, *PCDH10*,  
205 *TMEM51* and *IRX1* loci. The most prominent genetic association with RS was  
206 discovered in the *ADRA2A* locus. Furthermore, this association was significant  
207 independently in all cohorts, highlighting the significance of *ADRA2A* in RS. *In silico*  
208 follow-up analysis of *ADRA2A* RNA expression across tissues showed the highest  
209 expression in tibial arteries, and single cell expression analysis further supported the  
210 role of SMCs as the key cell type for *ADRA2A* expression. Finally, functional contraction  
211 assay in SMCs in cold conditions showed lower contraction in *ADRA2A*-deficient and  
212 higher contraction in *ADRA2A* overexpressing SMCs. Overall, our findings indicate  
213 *ADRA2A* in RS and as a regulator of vascular contraction in SMCs in temperature  
214 dependent fashion.

215 The strongest association in this study is a robust signal from *ADRA2A* in all four  
216 cohorts and with the same lead signals across cohorts. Furthermore, the lead variants  
217 are located in a regulatory region that affected *ADRA2A* expression in distal arteries in  
218 particular. In addition, we identified a specific subpopulation of SMCs that specifically  
219 expresses the  $\alpha_{2A}$ -adrenergic receptor. While the adrenergic system has been  
220 suggested as a potential pathological mechanism underlying RS<sup>[23,24,26,27,33-41](#)</sup>, these  
221 earlier studies have focused almost solely on the  $\alpha_{2C}$ -adrenergic receptor. Interestingly,  
222 a recent biobank study has identified some of the same RS loci<sup>[42](#)</sup>. In this study, we  
223 assessed contraction SMCs after *ADRA2A* or *ADRA2C* siRNA knockdown in human



224 SMCs. We saw a robust contraction upon cold with *ADRA2A* knockdown whereas  
225 *ADRA2C* silencing did not attenuate cold induced contraction in a similar manner to  
226 *ADRA2A*. Overall, these findings suggest an independent role of *ADRA2A* in vascular  
227 contraction and in temperature-dependent control of vascular tone.

228 In cold or stress conditions, norepinephrine and epinephrine are released and bind to  
229 adrenergic receptors throughout the body, which exerts various effects: dilating pupils  
230 and bronchioles, increase in heart rate, and in blood vessels constriction. The blood  
231 vessels constriction is mediated by the SMC that express adrenergic receptors on their  
232 surface. In healthy patients without RS, there are mechanisms to prevent unwanted and  
233 excessive vessel contraction. First, the cell constriction (upon cold or stress) can be  
234 limited by the increased release of ligand by translocation of the  $\alpha_{2C}$ -adrenergic receptor  
235 from the cytosol to the cell surface. Second,  $\alpha_{2A}$ -adrenergic receptors are also  
236 expressed on the presynaptic membrane and function there as a negative feedback  
237 loop for catecholamine release<sup>43</sup>.

238 Based on our results we propose a new model explaining the pathomechanism of RS  
239 that underlines the power of human genetics driven studies for understanding disease  
240 mechanisms. Our SMC contraction assays show that cold induced SMC contractility  
241 was modified by *ADRA2A* expression. Furthermore, we combined functional studies  
242 with the genomics-driven discovery that genetic variation at the *ADRA2A* locus leads to  
243 increased expression of  $\alpha_{2A}$ -adrenergic receptor in a population of SMCs. Such an  
244 increase in *ADRA2A* expression may sensitize these cells to adrenergic response and  
245 lead to increased signaling through the adrenergic pathway (Figure 6).

246 In addition to the signal from the adrenergic system, our meta-analysis indicated other  
247 signals and in particular endothelial nitric oxide synthase (eNOS) that clarify the  
248 pathological mechanisms with RS. Nitric oxide itself is a well-known mediator of  
249 vasodilation in arteries<sup>44</sup>. Therefore, it has been suggested as one of the underlying  
250 pathological mechanisms in RS although the role of it is still unclear<sup>2,45,46</sup>. These genetic  
251 associations may also elucidate the more specific disease mechanisms or even provide  
252 insight into the heterogeneity of the symptomatology in RS. For example, the signal  
253 from chromosome 6, HLA class I region, points towards the possible immune, infectious  
254 or autoimmune mechanisms in RS. It is still unclear, however, if this signal is a signal  
255 from autoimmune diseases that have secondary RS and not primary Raynaud's disease  
256 per se<sup>47,48</sup>, which was also indicated by Hartmann *et al.* (2023) in the UKB<sup>42</sup>. As for the  
257 other signals detected by our meta-analysis, *IRX1* gene has been implied in the  
258 embryonic development and in the development of fingers and digits which are affected  
259 in RS<sup>49,50</sup> as well as a tumor suppression gene<sup>51-54</sup>. Variants in *ACVR2A*, *RAB6C*,  
260 *PCDH10* and *TMEM51* have been implied in immunological traits, cell cycle,  
261 neurological disease and contractile function in cardio myocytes, respectively<sup>21,55-57</sup>.

262 Our study should be interpreted within the following limitations. Only a subset of  
263 individuals with RS have symptoms that are recognized or need treatment and we are  
264 likely missing the more benign spectrum of symptoms in the current population. Our  
265 findings are limited to individuals with European ancestry. Finally, data from  
266 subcutaneous microvascular cells or microvascular cells from RS patients were not  
267 available for this study and any genetic or expression effects might be accentuated or  
268 changed after disease onset in RS patients.

269 To summarize, we report here a robust association with *ADRA2A* with functional follow-  
270 up of this locus. In addition, we discovered seven loci that can be followed up in future  
271 functional studies. Our findings not only point towards the vascular pathophysiology  
272 underlying RS, but also specifically to the dysfunction of the autonomic nervous system  
273 and its dialogue with the vascular structure. Our results also suggest that the  
274 pathophysiological RS phenotype can be mediated through multiple possibly additive  
275 mechanisms involving adrenergic signaling, immune mechanisms and nitric oxide action  
276 and are in agreement with earlier studies. We highlight *ADRA2A* in the adrenergic  
277 system as a likely causal gene in a subset of microvascular SMCs, where we suggest it  
278 sensitizes these cells for catecholamines. Due to its localized expression in this subset  
279 of cells and the dose-dependent nature of the pathological phenotype as demonstrated  
280 by the genetic data, *ADRA2A* may be a promising target for further pharmaceutical  
281 studies.

282

## 283 Materials and Methods

284

### 285 Genetic analyses

286

#### 287 Cohorts

288

289 FinnGen is a public-private partnership registry-based study of Finnish residents  
290 combining genetic and electronic health record data from different registers, for example,  
291 primary care and hospital in- and out-patient visits. The release 10 (R10) contains data  
292 on up to 412,181 participants, primarily of Finnish ancestry from newborns to the age of

293 104 at baseline recruitment. The aim of the study is to collect the data of 500,000 Finns  
294 representing 10% of the population of Finland (for more information see  
295 <https://www.finngen.fi/en>).

296 The UK Biobank (UKB) is a population-based study containing over 500,000 individuals  
297 of mainly European ancestry<sup>58</sup>. The participants were recruited to the study between 2006  
298 to 2010, were aged between 37 to 73 years of age and were residents of the United  
299 Kingdom. The study is a combination of, for example, different lifestyle measures,  
300 genotypes, electronic health record data, blood count data and questionnaire data, and  
301 the data is updated frequently to capture the health trajectories of participated individuals.

302 The Estonian Biobank is a population-based biobank with 212,955 participants in the  
303 current data freeze (2023v1). All biobank participants have signed a broad informed  
304 consent form and information on ICD-10 codes is obtained via regular linking with the  
305 national Health Insurance Fund and other relevant databases, with majority of the  
306 electronic health records having been collected since 2004<sup>59</sup>.

307 The Mass-General Brigham (MGB) Biobank (formerly Partners HealthCare Biobank) is  
308 a hospital-based cohort study from the MGB healthcare network in Boston (MA, USA)  
309 with electronic health record (EHR), genetic, and lifestyle data<sup>60-62</sup>. The MGB Biobank  
310 includes data obtained from patients in several community-based primary care facilities  
311 and specialty tertiary care centers in Boston, MA<sup>60,63</sup>.

312 Ethics statement

313

314 Patients and control subjects in FinnGen provided informed consent for biobank  
315 research, based on the Finnish Biobank Act. Alternatively, separate research cohorts,  
316 collected prior the Finnish Biobank Act came into effect (in September 2013) and start  
317 of FinnGen (August 2017), were collected based on study-specific consents and later  
318 transferred to the Finnish biobanks after approval by Fimea (Finnish Medicines  
319 Agency), the National Supervisory Authority for Welfare and Health. Recruitment  
320 protocols followed the biobank protocols approved by Fimea. The Coordinating Ethics  
321 Committee of the Hospital District of Helsinki and Uusimaa (HUS) statement number for  
322 the FinnGen study is Nr HUS/990/2017.

323 The FinnGen study is approved by Finnish Institute for Health and Welfare (permit  
324 numbers: THL/2031/6.02.00/2017, THL/1101/5.05.00/2017, THL/341/6.02.00/2018,  
325 THL/2222/6.02.00/2018, THL/283/6.02.00/2019, THL/1721/5.05.00/2019 and  
326 THL/1524/5.05.00/2020), Digital and population data service agency (permit numbers:  
327 VRK43431/2017-3, VRK/6909/2018-3, VRK/4415/2019-3), the Social Insurance  
328 Institution (permit numbers: KELA 58/522/2017, KELA 131/522/2018, KELA  
329 70/522/2019, KELA 98/522/2019, KELA 134/522/2019, KELA 138/522/2019, KELA  
330 2/522/2020, KELA 16/522/2020), Findata permit numbers THL/2364/14.02/2020,  
331 THL/4055/14.06.00/2020, THL/3433/14.06.00/2020, THL/4432/14.06/2020,  
332 THL/5189/14.06/2020, THL/5894/14.06.00/2020, THL/6619/14.06.00/2020,  
333 THL/209/14.06.00/2021, THL/688/14.06.00/2021,  
334 THL/1284/14.06.00/2021, THL/1965/14.06.00/2021, THL/5546/14.02.00/2020 and

335 Statistics Finland (permit numbers: TK-53-1041-17 and TK/143/07.03.00/2020 (earlier  
336 TK-53-90-20)).

337 The Biobank Access Decisions for FinnGen samples and data utilized in FinnGen Data  
338 Freeze7 include: THL Biobank BB2017\_55, BB2017\_111, BB2018\_19, BB\_2018\_34,  
339 BB\_2018\_67, BB2018\_71, BB2019\_7, BB2019\_8, BB2019\_26, BB2020\_1, Finnish Red  
340 Cross Blood Service Biobank 7.12.2017, Helsinki Biobank HUS/359/2017, Auria  
341 Biobank AB17-5154 and amendment #1 (August 17 2020), Biobank Borealis of  
342 Northern Finland\_2017\_1013, Biobank of Eastern Finland 1186/2018 and amendment  
343 22 § /2020, Finnish Clinical Biobank Tampere MH0004 and amendments (21.02.2020  
344 06.10.2020), Central Finland Biobank 1-2017, and Terveystalo Biobank STB  
345 2018001.2.

346 The activities of the EstBB are regulated by the Human Genes Research Act, which  
347 was adopted in 2000 specifically for the operations of the EstBB. Individual level data  
348 analysis in the EstBB was carried out under ethical approval 1.1-12/624 from the  
349 Estonian Committee on Bioethics and Human Research (Estonian Ministry of Social  
350 Affairs), using data according to release application 6-7/GI/16279 from the Estonian  
351 Biobank.

352 The North West Multi-centre Research Ethics Committee (MREC) has granted the  
353 Research Tissue Bank (RTB) approval for the UKB that covers the collection and  
354 distribution of data and samples (<http://www.ukbiobank.ac.uk/ethics/>). Our work was  
355 performed under the UKB application number 22627 (Principal Investigator Dr Matti  
356 Pirinen, FIMM). All participants included in the conducted analyses have given a written  
357 consent to participate.

358 The MGB has obtained a Certificate of Confidentiality. In addition, The MGB works in  
359 close collaboration with the Partners Human Research Committee (PHRC) (the  
360 Institutional Review Board). This collaboration has ensured that the Biobank's actions and  
361 procedures meet the ethical standards for research with human subjects. Biobank  
362 patients are recruited from inpatient stays, emergency department settings, outpatient  
363 visits, and electronically through a secure online portal for patients. Recruitment and  
364 consent materials are fully translated in Spanish to promote patient inclusion. The  
365 systematic enrollment of patients across the MGB network and the active inclusion of  
366 patients from diverse backgrounds contribute to a Biobank reflective of the overall  
367 demographic of the population receiving care within the MGB network. Recruitment for  
368 the Biobank launched in 2009 and is ongoing through both in-person recruitment at  
369 participating clinics and electronically through the patient portal. The recruitment strategy  
370 has been described previously<sup>60</sup>. All recruited patients provided written consent upon  
371 enrollment, and are offered an option to refuse consent.

372

### 373 Genotyping and quality control

374

375 Genotyping in the FinnGen cohort was performed by using Illumina (Illumina Inc., San  
376 Diego, CA, USA) and Affymetrix arrays (Thermo Fisher Scientific, Santa Clara, CA,  
377 USA) and lifted over to build version 38 (GRCh38/hg38)<sup>64</sup>. Individuals with high  
378 genotype absence (> 5%), inexplicit sex or excess heterozygosity (+-4 standard  
379 deviations) were excluded from the data<sup>64</sup>. Additionally, variants that had high absence  
380 (> 2%), low minor allele count (< 3) or low Hardy-Weinberg Equilibrium (HWE) ( $P <$

381  $1 \times 10^{-06}$ ) were removed. More detailed explanations of the genotyping, quality control  
382 and the genotype imputation are provided elsewhere<sup>64</sup>. All individuals in the cohort were  
383 Finns and matched against the SiSu v4 reference panel (<http://www.sisuproject.fi/>).

384 All the EstBB participants have been genotyped at the Core Genotyping Lab of the  
385 Institute of Genomics, University of Tartu, using Illumina Global Screening Array  
386 v3.0\_EST. Samples were genotyped and PLINK format files were created using Illumina  
387 GenomeStudio v2.0.4. Individuals were excluded from the analysis if their call-rate was  
388  $< 95\%$ , if they were outliers of the absolute value of heterozygosity ( $> 3SD$  from the  
389 mean) or if sex defined based on heterozygosity of X chromosome did not match sex in  
390 phenotype data. Before imputation, variants were filtered by call-rate  $< 95\%$ , HWE P-  
391 value  $< 1 \times 10^{-04}$  (autosomal variants only), and minor allele frequency  $< 1\%$ . Genotyped  
392 variant positions were in build 37 and were lifted over to build 38 using Picard. Phasing  
393 was performed using the Beagle v5.4 software<sup>65</sup>. Imputation was performed with Beagle  
394 v5.4 software (beagle.22Jul22.46e.jar) and default settings. Dataset was split into  
395 batches 5,000. A population specific reference panel consisting of 2,695 WGS samples  
396 was utilized for imputation and standard Beagle hg38 recombination maps were  
397 used. Based on principal component analysis, samples who were not of European  
398 ancestry were removed. Duplicate and monozygous twin detection was performed with  
399 KING 2.2.7<sup>66</sup>, and one sample was removed out of the pair of duplicates. Analyses were  
400 restricted to individuals with European ancestry.

401 The UKB genotyped 488,477 participants: 49,950 on the Affymetrix (Thermo Fisher  
402 Scientific) UK BiLEVE Axiom Array and 438,427 on the highly similar Affymetrix UK  
403 Biobank Axiom Array, These arrays captured up to 825,927 SNPs and short indels, with



404 variants prioritized for known coding variants, those previously associated with disease  
405 and ancestry-specific markers that provide a good imputation backbone. DNA was  
406 extracted from blood samples taken at baseline interviews, between 2006 and 2010,  
407 and genotyping was carried out in 106 sequential batches, giving genotype calls for  
408 812,428 unique variants in 489,212 participants. After removing high missingness and  
409 very rare variants, as well as poor-quality samples, these genotypes were phased using  
410 SHAPEIT3 and imputed to the Haplotype Reference Consortium (HRC) and to a  
411 merged UK10K and 1000 Genomes phase 3 reference panel<sup>67</sup>, both in genome  
412 assembly GRCh37 using IMPUTE2. This resulted in 93,095,623 autosomal SNPs, short  
413 indels and large structural variants in 487,442 individuals and 3,963,705 markers on the  
414 X chromosome. For more details, see Bycroft *et al.* 2018<sup>58</sup>.

415 The MGB genotyped 53,297 participants on the Illumina Global Screening Array ('GSA')  
416 and 11,864 on Illumina Multi-Ethnic Global Array ("MEG"). The GSA arrays captured  
417 approximately 652K SNPs and short indels, while the MEG arrays captured  
418 approximately 1.38M SNPs and short indels. These genotypes were filtered for high  
419 missingness ( $> 2\%$ ) and variants out of HWE ( $P < 1 \times 10^{-12}$ ), as well as variants with an  
420 AF discordant ( $P < 1 \times 10^{-150}$ ) from a synthesized AF calculated from GnomAD  
421 subpopulation frequencies and a genome wide GnomAD model fit of the entire cohort.  
422 This resulted in approximately 620K variants for GSA and 1.15M for MEG. The two sets  
423 of genotypes were then separately phased and imputed on the TOPMed imputation  
424 server (Minimac4 algorithm) using the TOPMed r2 reference panel. The resultant  
425 imputation sets were both filtered at an  $R^2 > 0.4$  and a  $MAF > 0.001$ , and then the two  
426 sets were merged/intersected resulting in approximately 19.5M GRCh38 autosomal

427 variants. The sample set for analysis here was then restricted to just those classified as  
428 EUR (N = 54,452) according to a metric of being +/- 2 SDs of the average EUR  
429 sample's principal components 1 to 4 in the HGDP reference panel.

430

### 431 Phenotype definition

432

433 We built the phenotype for RS using ICD10 code I73.0 in all of our cohorts (see Suppl.  
434 Table 1 for the total number of cases and controls in each cohort used). Additionally, we  
435 used the self-reported measures and primary care codes of RS in the UKB, and the  
436 ICD-9 code 4430 in the FinnGen R10 and the UKB.

437 For FinnGen R10 phenotype definition, we used both the hospital record data (inpatient  
438 N = 88 (4.2%) cases and outpatient N = 1,204 (57.8%) cases) and primary care data (N  
439 = 792 (38.0%)). Most of the cases (N = 2,025 (87.75%)) in the EstBB were from primary  
440 care data setting, and the rest were from hospital record data (N = 180 (12.25%)). In the  
441 case of MGB, all the cases were obtained from hospital record data (inpatient N = 251  
442 (13.2%) cases and outpatient N = 1,656 (86.8%) cases).

443 From the UKB data, we obtained both self-reported and electronic health record data for  
444 disease definitions. To define the phenotypes, we used data from the self-report non-  
445 cancer illness codes (data field 20002), which were assessed during the baseline  
446 interview, hospital inpatient records (HES; data field 41234) and primary care diagnosis  
447 records (data field 42040). For RS, code 1561 was used from the self-reported data.

448 From the hospital inpatient data, we included individuals as a case for the phenotype if  
449 they had I73.0 ICD-10 or 4430 ICD-9 diagnosis code. In the primary care data,

450 diagnoses are coded using the NHS-specific Read v2 or CTV3 codes instead of the  
451 ICD-coding. We used the following Read codes to define the respective phenotype:

452 - Read v2: “G730.”, “G7301”, “G7300” or “G730z”

453 - Read CTV3 (v3): “G730.”, “XE0VQ”, “G7300”, “G730z”, “G7301”, “X7051” or  
454 “XE0XA”

455 With this definition for RS, we ended up with 5,162 cases and 440,833 controls of  
456 European ancestry. Most of the cases for RS came from the primary care data (N =  
457 2,953 (57.2%)) and hospital inpatient data (N = 1,664 (32.2%)).

458 Overall, of our RS cases 5,770 (50.8%) come from primary care data, 5,043 (44.4%)  
459 from hospital record data and 545 (4.8%) from self-reported data. Individuals who did  
460 not have the codes mentioned above were used as controls.

461

## 462 GWAS

463

464 For the FinnGen cohort, GWAS was conducted using the REGENIE (v.2.2.4) pipeline  
465 for R10 data<sup>68</sup> (<https://github.com/FINNGEN/regenie-pipelines>). Analysis was adjusted  
466 for age at death or end of follow up (12.31.2021), sex, genotyping batches and the first  
467 10 genetic principal components. Firth approximation was applied for variants with  
468 association P-value < 0.01.

469 The UKB GWA analyses were performed using REGENIE v3.1.1<sup>68</sup>. The whole-genome  
470 regression model (step 1) was created using 524,307 high-quality genotyped SNPs (bi-  
471 allelic; MAF ≥ 1%; HWE P > 1x10<sup>-06</sup>; present in all genotype batches, total missingness

472 < 1.5% and not in a region of long-range LD<sup>69</sup> with the leave-one-chromosome-out (--  
473 loocv) option enabled. We corrected for the following covariates:

- 474 - age at follow-up end (2019.08.18) or death (if earlier than follow-up end),  
475 calculated as the difference in years between the 15th day of month and year of  
476 birth (data fields 52 and 34, respectively) and the follow-up end or death date.
- 477 - sex (data field 31)
- 478 - genotyping array (categorical), derived from genotyping batch (data field 20000),  
479 as “UKB BiLEVE” (batches -11 to -1), “UKB Axiom release 1” (1 to 22) and “UKB  
480 Axiom release 2” (23 to 95).
- 481 - genetic principal components 1 to 10 (data field 22009)
- 482 - centre of baseline visit (categorical; data field 54)

483 The GWA (step 2) was performed using v3 imputed genotypes<sup>58</sup> for chromosomes 1-22  
484 and X with the approximate Firth correction applied for variants with association P-value  
485 < 0.05 (default setting), using the flags --firth, --approx and --firth-se. After analysis with  
486 REGENIE, we excluded results for imputed variants with MAF < 0.1% and/or imputation  
487 INFO < 0.3.

488 Association analysis in the EstBB was carried out for all variants with an INFO score >  
489 0.4 using the additive model as implemented in REGENIE v3.0.3 with standard binary  
490 trait settings<sup>68</sup>. Logistic regression was carried out with adjustment for current age, age<sup>2</sup>,  
491 sex and 10 first genetic principal components as covariates, analyzing only variants with  
492 a minimum minor allele count of 2.

493 In the MGB, the association analysis was carried out using REGENIE v3.2.2<sup>68</sup>, with  
494 covariates of Age, Sex, Genotype-Chip and five first principal components of ancestry  
495 calculated on just the analysis set (EUR only) of samples, analyzing only variants with a  
496 minimum minor allele count of 10.

497 Manhattan-plots for all the cohorts' GWASs and meta-analyses were plotted using R  
498 version 4.0.1 (packages: qqman and RColorBrewer).

499

## 500 Meta-analysis

501

502 Meta-analyses were conducted using METAL

503 ([https://genome.sph.umich.edu/wiki/METAL\\_Documentation](https://genome.sph.umich.edu/wiki/METAL_Documentation)) with standard settings,

504 and tracking allele frequency with the AVERAGEFREQ option and analyzing

505 heterogeneity between used summary statistics with the ANALYZE HETEROGENEITY

506 option. Summary statistics from different cohorts were matched against rsIDs. Both

507 sample size based meta-analysis and effect estimate based analyses were run (Figure

508 1, Table 1 & Suppl. Table 3). Locus zoom plots from the meta-analysis results were

509 created using the LocusZoom web browser (<https://github.com/statgen/locuszoom>)<sup>70</sup>.

510

## 511 eQTL and co-localization analyses

512

513 We conducted the eQTL analysis by using the web browser of the GTEx project

514 (<https://gtexportal.org/home/>)<sup>71</sup>. Co-localization analyses were performed using the

515 coloc R package (v5.1.0.1)<sup>72,73</sup> in R v4.2.2. We extracted all variants in a 200kb region

516 centered on the lead variant and imported the same region from GTEx v8<sup>71</sup> eQTL  
517 association statistics. We then tested the co-localization between RS and each of the 49  
518 tissues and generated co-localization plots using the LocusCompareR R package  
519 (v1.0.0)<sup>74</sup> using LD  $r^2$  from 1000 Genomes European-ancestry samples.

520

## 521 Functional assays

522

### 523 RNA extraction and RT-PCR

524

525 RNA was isolated according to manufacturer's instructions using RNeasy plus micro kit  
526 (Qiagen, #74034). The quality of the RNA was determined with Nanodrop ND-1000  
527 (Thermo Fisher Scientific), and 500 ng of total RNA was used for cDNA synthesis using  
528 High-capacity RNA-to-cDNA kit (Life Technologies, #4388950) on a BIO-RAD C1000  
529 thermal cycler. RT-qPCR was performed using Taqman probes for *ADRA2A*  
530 (Hs01099503), *ADRA2C* (Hs03044628) and *NOTCH3* (Hs01128537) according to the  
531 manufacturer's instructions on a ViiA7 Real-Time PCR system (Applied Biosystems,  
532 Foster City, CA). GAPDH and UBC were used to normalize relative expression levels.  
533 The  $2^{-\Delta\Delta C_t}$  method was used to quantify relative gene expression levels. Technical  
534 triplicates of  $C_t$  values were averaged for each sample and normalized to the  
535 housekeeping gene. Expression levels of mRNA are presented as fold change (control  
536 group = 1).

537 SiRNA and lentiviral overexpression

538

539 For siRNA transfection, cells were 60% confluent when treated with siRNA or scramble  
540 control to a final concentration of 20 nM with RNAiMax (Invitrogen, Carlsbad, CA). The  
541 siRNAs for *ADRA2A* (Cat # L-005422-00-0005) and *ADRA2C* (Cat # L-005424-00-0005)  
542 were purchased from Dharmacon (ONTARGET plus SMART pool siRNA). Cells were  
543 treated with an equimolar combination of Silencer and Scramble and collected 72 hours  
544 after transfection.

545 For overexpression studies *ADRA2A* (Human Tagged ORF Clone in pLenti-C-Myc-DDK  
546 Lentiviral Gene Expression Vector, NM\_000681) and *ADRA2C* (Human Tagged ORF  
547 Clone in pLenti-C-Myc-DDK Lentiviral Gene Expression Vector, NM\_000683) plasmids  
548 were purchased from OriGene Technologies. To package viruses  $8.5 \times 10^5$  HEK293T cells  
549 plated in each well of a six-well plate. The following day, lentiviral gene expression vectors  
550 were co-transfected with second generation lentivirus packaging plasmids, pMD2.G and  
551 pCMV-dR8.91, into cells using Lipofectamine 3000 (Thermo Fisher, L3000015) according  
552 to the manufacturer's instructions. ViralBoost Reagent (AllStem Cell Advancements,  
553 VB100) was added (1:500) with fresh media after 5 hours. Supernatant containing viral  
554 particles was collected 48 hours after transfection and filtered. PSMCs were transduced  
555 with high MOI and treated for 12 hours and collected 72 hours after transfection.

556 RNAscope

557

558 Frozen sections of human coronary arteries were processed according to the

559 manufacturer's instructions, and all reagents were obtained from ACD Bio (Newark, CA).

560 Sections were incubated with commercially available probes against human *ADRA2A*

561 (#602791). Colorimetric assays were performed per the manufacturer's instructions.

562

563 Single-cell RNA sequencing (scRNAseq) from human tissue

564

565 scRNAseq data was obtained from the human vascular atlas available on

566 <https://cellxgene.cziscience.com/>.

567

568 Smooth muscle cell contraction assay

569

570 Pulmonary arterial SMCs were transfected with either scrambled siRNA or siADRA2A,

571 siADRA2C or combination of both. Following 48 hours of transfection, cells were

572 trypsinized and collected to be used for a collagen-based cell contraction assay Cyto-

573 Select 48-well Cell Contraction Assay Kit (Cell Biolabs, San Diego, CA). In the assay, a

574 mixture the pulmonary SMCs ( $3 \times 10^6$ /ml) and cold Collagen Gel Working Solution was

575 incubated in a 48-well dish at 37°C for 1 hour to induce optimal polymerization following

576 the manufacturer's instructions. Next, cell culture medium with added SMC contraction

577 agent or without was added on top of each well already containing the polymerized cell

578 and collagen mixture. The cells were then incubated at either 28 °C or at 37°C, 5% CO<sub>2</sub>.



579 After 48 hours, the Keyence slide scanning microscope BZ-X810 was used to image the  
580 wells and cell contraction was measured using ImageJ by drawing the outlines of the gel,  
581 calculating the gel area, and comparing it to the well area.

582

## 583 Generation and analysis of CRIPSR lines

584

585 Genome editing of the region around rs7090046 was performed by CRISPRi/dCas9-  
586 KRAB system as previously reported<sup>74</sup>. The guide RNAs targeting this SNP were  
587 designed using Benchling online tools. Synthesized oligos were then cloned into pBA904  
588 vector backbone containing dCas9-KRAB and lentiviruses was packaged as described  
589 above. For the CRISPR interference experiment, PSMCs cells were seeded into 6 well  
590 plate ( $8 \times 10^5$  cells /well). The next day, cells were transduced with the virus for 12 hours  
591 with 8  $\mu\text{g}/\text{mL}$  polybrene. The cells were cultured for an additional 5 days with medium  
592 change until RNA was extracted. GuideRNA sequences are listed in Supplementary  
593 Table 6.

594

## 595 Primary cell culture and sample processing

596

597 Primary human pulmonary artery smooth muscle cells (PASMC) obtained from Dr.  
598 Rabenovich were originally isolated from pulmonary arteries ( $< 1\text{mm}$ ) harvested from  
599 unused donor lungs all obtained de-identified from the Pulmonary Hypertension  
600 Breakthrough Initiative (<https://ipahresearch.org/phbi-research/>). For the experiments,  
601 total RNA was isolated from confluent cells at passage 5 and 6.

602

## 603 Statistics and reproducibility for the functional studies

604

605 All statistical analyses were conducted using GraphPad Prism software version 9  
606 (Dotmatics Inc). Difference between two groups were determined using an unpaired two-  
607 tailed Student's t-test. Differences between multiple groups were evaluated by one-way  
608 analysis of variance (ANOVA) followed by Dunnett's post-hoc test after the sample  
609 distribution was tested for normality. P-values < 0.05 were considered statistically  
610 significant. All error bars represent standard error of the mean. Number of stars for the P-  
611 values in the graphs: \*\*\* P < 0.001; \*\* P < 0.01; \* P < 0.05. No statistical method was  
612 used to predetermine sample size, which was based on extensive prior experience with  
613 this model.

614

## 615 Data and code availability

616

617 Individual-level data for can be accessed on successful application for cohorts used in  
618 this study. The FinnGen individual level data may be accessed through applications to  
619 the Finnish Biobanks' FinnBB portal, Fingenuous ([www.finbb.fi](http://www.finbb.fi)). For the individual level  
620 data of theUKB, applications can be made through the UKB portal at  
621 <https://www.ukbiobank.ac.uk/enable-your-research/apply-for-access>. For MGB,  
622 individual level data are available from the Mass General Brigham Human Research  
623 Office/Institutional Review Board at Mass General Brigham (contact located at

624 [https://www.partners.org/Medical-Research/Support-Offices/Human-Research-](https://www.partners.org/Medical-Research/Support-Offices/Human-Research-Committee-IRB/Default.aspx)  
625 [Committee-IRB/Default.aspx](https://www.partners.org/Medical-Research/Support-Offices/Human-Research-Committee-IRB/Default.aspx)) for researchers who meet the criteria for access to  
626 confidential data. Lastly, for the EstBB, preliminary inquiries to access individual level  
627 data for scientific research can be sent to [releases@ut.ee](mailto:releases@ut.ee).

628 Summary level data will be available upon publication in Dryad open-access repository.

629

## 630 Conflicts of Interest

631

632 The authors declare no competing interests.

633

## 634 Acknowledgments

635

636 A.T. received support for this work from the Instrumentarium Science Foundation  
637 (230041) and Doctoral Programme Brain and Mind (University of Helsinki). A.T. and  
638 H.M.O. received support from the Academy of Finland (340539). Additionally, M.R.  
639 received support from Sigrid Juselius Foundation, Emil Aaltonen foundation, Biomedicum  
640 Helsinki Foundation, Orion Research Foundation and from Finnish Foundation for  
641 Cardiovascular Research.

642 We want to acknowledge the FinnGen study and the FinnGen team for their contribution.

643 We would like to thank the UK Biobank and the Mass General Brigham Biobank

644 participants and staff for making this work possible. We also want to acknowledge the

645 participants of the Estonian Biobank for their contributions. The Estonian Genome Center  
646 analyses were partially carried out in the High Performance Computing Center, University  
647 of Tartu.

648 The FinnGen project is funded by two grants from Business Finland (HUS 4685/31/2016  
649 and UH4386/31/2016) and the following industry partners: AbbVie Inc., AstraZeneca UK  
650 Ltd, BiogenMA Inc., Bristol Myers Squibb, Genentech Inc., Merck Sharp Dohme Corp,  
651 Pfizer Inc., Glaxo-SmithKline Intellectual Property Development Ltd., Sanofi US  
652 Services Inc., Maze Therapeutics Inc., Janssen Biotech Inc, Novartis Pharma AG, and  
653 Boehringer Ingelheim. Following biobanks are acknowledged for delivering biobank  
654 samples to FinnGen: Auria Biobank ([www.auria.fi/biopankki](http://www.auria.fi/biopankki)), THL Biobank  
655 ([www.thl.fi/biobank](http://www.thl.fi/biobank)), Helsinki Biobank ([www.helsinginbiopankki.fi](http://www.helsinginbiopankki.fi)), Biobank Borealis of  
656 Northern Finland ([https://www.ppshep.fi/Tutkimus-ja-opetus/Biopankki/Pages/Biobank-](https://www.ppshep.fi/Tutkimus-ja-opetus/Biopankki/Pages/Biobank-Borealis-briefly-in-English.aspx)  
657 [Borealis-briefly-in-English.aspx](https://www.ppshep.fi/Tutkimus-ja-opetus/Biopankki/Pages/Biobank-Borealis-briefly-in-English.aspx)), Finnish Clinical Biobank Tampere ([www.tays.fi/en-](http://www.tays.fi/en-US/Research/and/development/Finnish/Clinical/Biobank/Tampere)  
658 [US/Research/and/development/Finnish/Clinical/Biobank/Tampere](http://www.tays.fi/en-US/Research/and/development/Finnish/Clinical/Biobank/Tampere)), Biobank of Eastern  
659 Finland ([www.ita-suomenbiopankki.fi/en](http://www.ita-suomenbiopankki.fi/en)), Central Finland Biobank ([www.ksshp.fi/fi-](http://www.ksshp.fi/fi-FI/Potilaalle/Biopankki)  
660 [FI/Potilaalle/Biopankki](http://www.ksshp.fi/fi-FI/Potilaalle/Biopankki)), Finnish Red Cross Blood Service Biobank  
661 ([www.veripalvelu.fi/verenluovutus/biopankkitoiminta](http://www.veripalvelu.fi/verenluovutus/biopankkitoiminta)) and Terveystalo Biobank  
662 ([www.terveystalo.com/fi/Yritystietoa/Terveystalo-Biopankki/Biopankki/](http://www.terveystalo.com/fi/Yritystietoa/Terveystalo-Biopankki/Biopankki/)). All Finnish  
663 Biobanks are members of BBMRI.fi infrastructure ([www.bbmri.fi](http://www.bbmri.fi)) and FINBB biobank  
664 cooperative (<https://finbb.fi/>) is the coordinator of the BBMRI-ERIC operations in Finland  
665 covering all Finnish biobanks.

666 The work of the Estonian Genome Center, University of Tartu was funded by the  
667 European Union through Horizon 2020 research and innovation program under grants

668 no. 810645 and 894987, through the European Regional Development Fund projects  
669 GENTRANSMED (2014-2020.4.01.15-0012), MOBEC008, MOBERA21 and Estonian  
670 Research Council Grant PRG1291

## References

1. Mathias, C.J., Owens, A., Iodice, V. & Hakim, A. Dysautonomia in the Ehlers-Danlos syndromes and hypermobility spectrum disorders-With a focus on the postural tachycardia syndrome. *Am. J. Med. Genet. C. Semin. Med. Genet.* 187(4), 510-519 (2021).
2. Nawaz, I., Nawaz, Y., Nawaz, E., Manan, M.R. & Mahmood, A. Raynaud's Phenomenon: Reviewing the Pathophysiology and Management Strategies. *Cureus* 14(1), (2022).
3. Garner, R., Kumari, R., Lanyon, P., Doherty, M. & Zhang, W. Prevalence, risk factors and associations of primary Raynaud's phenomenon: systematic review and meta-analysis of observational studies. *BMJ Open* 5(3), (2015).
4. World Health Organization. (2004). ICD-10: international statistical classification of diseases and related health problems: tenth revision, 2nd ed. World Health Organization. <https://apps.who.int/iris/handle/10665/42980>
5. Mizuno, R., Fujimoto, S., Saito, Y. & Nakamura, S. Cardiac Raynaud's phenomenon induced by cold provocation as a predictor of long-term left ventricular dysfunction and remodelling in systemic sclerosis: 7-year follow-up study. *Eur. J. Heart Fail* 12(3), 268-275 (2010).
6. Xia, Y.K., Tu, S.H., Hu, Y.H., Wang, Y., Chen, Z., Day, H.T. & Ross, K. Pulmonary hypertension in systemic lupus erythematosus: a systematic review and analysis of 642 cases in Chinese population. *Rheumatol. Int.* 33(5), 1211-1217 (2013).
7. Vonk, M.C., Vandecasteele, E. & van Dijk, A.P. Pulmonary hypertension in connective tissue diseases, new evidence and challenges. *Eur. J. Clin. Invest.* 51(4), (2021).
8. Haque, A., Kiely, D.G., Kovacs, G., Thompson, A.A.R. & Condliffe, R. Pulmonary hypertension phenotypes in patients with systemic sclerosis. *Eur. Respir. Rev.* 30(161), (2021).
9. Denton, C. P. & Khanna, D. K. Systemic sclerosis. *Lancet* 390, 1685–1699 (2017).
10. Evans, M., Barry, M., Im, Y., Brown, A. & Jason, L.A. An investigation of symptoms predating CFS onset. *J. Prev. Interv. Community* 43(1), 54-61 (2015).
11. Giuggioli, D., Spinella, A., de Pinto, M., Mascia, M.T. & Salvarani, C. From Raynaud Phenomenon to Systemic Sclerosis in COVID-19: A Case Report. *Adv. Skin Wound Care* 35(2), 123-124 (2022).
12. Curtiss, P., Svigos, K., Schwager, Z., Lo Sicco, K. & Franks Jr., A.G., Part I: Epidemiology, Pathophysiology, and Clinical Considerations of Primary and Secondary Raynaud's Phenomenon, *Journal of the American Academy of Dermatology* (2022).
13. Cherkas, L.F., Williams, F.M., Carter, L., Howell, K., Black, C.M., Spector, T.D. & MacGregor, A.J. Heritability of Raynaud's phenomenon and vascular

- responsiveness to cold: a study of adult female twins. *Arthritis Rheum.* 57(3), 524-528 (2007).
14. Hur, Y.M., Chae, J.H., Chung, K.W., Kim, J.J., Jeong, H.U., Kim, J.W., Seo, S.Y. & Kim, K.S. Feeling of cold hands and feet is a highly heritable phenotype. *Twin Res. Hum. Genet.* 15(2), 166-169 (2012).
  15. Maricq, H.R., Carpentier, P.H., Weinrich, M.C., Keil, J.E., Franco, A., Drouet, P., Ponçot, O.C. & Maines, M.V. Geographic variation in the prevalence of Raynaud's phenomenon: Charleston, SC, USA, vs Tarentaise, Savoie, France. *J. Rheumatol.* 20(1), 70-76 (1993).
  16. Zülch, A., Becker, M.B. & Gruss, P. Expression pattern of *Irxa1* and *Irxa2* during mouse digit development. *Mech. Dev.* 106(1-2), 159-162 (2001).
  17. Klarin, D., Lynch, J., Aragam, K., Chaffin, M., Assimes, T.L., Huang, J., Lee, K.M., Shao, Q., Huffman, J.E., Natarajan, P., et al. Genome-wide association study of peripheral artery disease in the Million Veteran Program. *Nat. Med.* 25(8), 1274-1279 (2019).
  18. Chen, K., Pittman, R.N. & Popel, A.S. Nitric oxide in the vasculature: where does it come from and where does it go? A quantitative perspective. *Antioxid Redox Signal.* 10(7), 1185-1198 (2008).
  19. Luiking, Y.C., Ten Have, G.A., Wolfe, R.R. & Deutz, N.E. Arginine de novo and nitric oxide production in disease states. *Am. J. Physiol. Endocrinol. Metab.* 303(10), 1177-1189 (2012).
  20. Bleakley, C., Hamilton, P.K., Pumb, R., Harbinson, M. & McVeigh, G.E. Endothelial Function in Hypertension: Victim or Culprit? *J. Clin. Hypertens. (Greenwich)* 17(8), 651-654 (2015).
  21. Astle, W.J., Elding, H., Jiang, T., Allen, D., Ruklisa, D., Mann, A.L., Mead, D., Bouman, H., Riveros-Mckay, F., Kostadima, M.A., et al. The Allelic Landscape of Human Blood Cell Trait Variation and Links to Common Complex Disease. *Cell* 167(5), 1415-1429 (2016).
  22. Zhu, Z., Wang, X., Li, X., Lin, Y., Shen, S., Liu, C.L., Hobbs, B.D., Hasegawa, K., Liang, L., International COPD Genetics Consortium, Boezen, H.M., Camargo, C.A. Jr., Cho, M.H. & Christiani, D.C. Genetic overlap of chronic obstructive pulmonary disease and cardiovascular disease-related traits: a large-scale genome-wide cross-trait analysis. *Respir. Res.* 20(1), (2019).
  23. Reid, J.L. Alpha-adrenergic receptors and blood pressure control. *Am. J. Cardiol.* 57(9), 6-12 (1986).
  24. Altman, J.D., Trendelenburg, A.U., MacMillan, L., Bernstein, D., Limbird, L., Starke, K., Kobilka, B.K. & Hein, L. Abnormal regulation of the sympathetic nervous system in alpha2A-adrenergic receptor knockout mice. *Mol. Pharmacol.* 56(1), 154-161 (1999).
  25. Dinunno, F.A., Eisenach, J.H., Dietz, N.M. & Joyner, M.J. Post-junctional alpha-adrenoceptors and basal limb vascular tone in healthy men. *J. Physiol.* 540(Pt 3), 1103-1110 (2002).

26. Chotani, M.A., Mitra, S., Su, B.Y., Flavahan, S., Eid, A.H., Clark, K.R., Montague, C.R., Paris, H., Handy, D.E. & Flavahan, N.A. Regulation of alpha(2)-adrenoceptors in human vascular smooth muscle cells. *Am. J. Physiol. Heart Circ. Physiol.* 286(1), 59-67 (2004).
27. Brum, P.C., Hurt, C.M., Shcherbakova, O.G., Kobilka, B. & Angelotti, T. Differential targeting and function of alpha2A and alpha2C adrenergic receptor subtypes in cultured sympathetic neurons. *Neuropharmacology* 51(3), 397-413 (2006).
28. Kurnik, D., Muszkat, M., Li, C., Sofowora, G.G., Friedman, E.A., Scheinin, M., Wood, A.J. & Stein, C.M. Genetic variations in the  $\alpha(2A)$ -adrenoreceptor are associated with blood pressure response to the agonist dexmedetomidine. *Circ. Cardiovasc. Genet.* 4(2), 179-187 (2011).
29. Docherty, JR. Subtypes of functional alpha1- and alpha2-adrenoceptors. *Eur. J. Pharmacol.* 361(1), 1-15 (1998).
30. ENCODE Project Consortium. An integrated encyclopedia of DNA elements in the human genome. *Nature* 489(7414), 57-74 (2012).
31. Villa, N., Walker, L., Lindsell, C.E., Gasson, J., Iruela-Arispe, M.L. & Weinmaster, G. Vascular expression of Notch pathway receptors and ligands is restricted to arterial vessels. *Mech. Dev.* 108(1-2), 161-164 (2001).
32. Liu, H., Zhang, W., Kennard, S., Caldwell, R.B. & Lilly, B. Notch3 is critical for proper angiogenesis and mural cell investment. *Circ. Res.* 107(7), 860-870 (2010).
33. Bailey, S.R., Eid, A.H., Mitra, S., Flavahan, S. & Flavahan, N.A. Rho kinase mediates cold-induced constriction of cutaneous arteries: role of alpha2C-adrenoceptor translocation. *Circ. Res.* 94(10), 1367-1374 (2004).
34. Bailey, S.R., Mitra, S., Flavahan, S. & Flavahan, N.A. Reactive oxygen species from smooth muscle mitochondria initiate cold-induced constriction of cutaneous arteries. *Am. J. Physiol. Heart Circ. Physiol.* 289(1), 243-250 (2005).
35. Freedman, R.R., Moten, M., Migály, P. & Mayes, M. Cold-induced potentiation of alpha 2-adrenergic vasoconstriction in primary Raynaud's disease. *Arthritis Rheum.* 36(5), 685-690 (1993).
36. Freedman, R.R., Baer, R.P. & Mayes, M.D. Blockade of vasospastic attacks by alpha 2-adrenergic but not alpha 1-adrenergic antagonists in idiopathic Raynaud's disease. *Circulation* 92(6), 1448-1451 (1998).
37. MacMillan, L.B., Hein, L., Smith, M.S., Piascik, M.T. & Limbird, L.E. Central hypotensive effects of the alpha2a-adrenergic receptor subtype. *Science* 273(5276), 801-803 (1996).
38. Chotani, M.A., Flavahan, S., Mitra, S., Daunt, D. & Flavahan, N.A. Silent alpha(2C)-adrenergic receptors enable cold-induced vasoconstriction in cutaneous arteries. *Am. J. Physiol. Heart Circ. Physiol.* 278(4), 1075-1083 (2000).
39. Jeyaraj, S.C., Chotani, M.A., Mitra, S., Gregg, H.E., Flavahan, N.A. & Morrison, K.J. Cooling evokes redistribution of alpha2C-adrenoceptors from Golgi to



- plasma membrane in transfected human embryonic kidney 293 cells. *Mol. Pharmacol.* 60(6), 1195-2000 (2001).
40. Chotani, M.A. & Flavahan, N.A. Intracellular  $\alpha(2C)$ -adrenoceptors: storage depot, stunted development or signaling domain? *Biochim. Biophys. Acta.* 1813(8), 1495-1503 (2011).
  41. Landry, G.J. Current medical and surgical management of Raynaud's syndrome. *J. Vasc. Surg.* 57(6), 1710-1716 (2013).
  42. Hartmann, S., Yasmeen, S., Jacobs, B.M, Denaxas, S., Pirmohamed, M., Gamazon, E.R., Caulfield, M.J, Genes & Health Research Team, Hemingway, H. & Pietzner, M., Langenberg, C. ADRA2A and IRX1 are putative risk genes for Raynaud's phenomenon. Preprint at medRxiv <https://doi.org/10.1101/2022.10.19.22281276> (2023).
  43. Langer, S.Z. Presynaptic regulation of the release of catecholamines. *Pharmacol. Rev.* 32(4), 337-362 (1980).
  44. Ahmad, A., Dempsey, S.K., Daneva, Z., Azam, M., Li, N., Li, P.L. & Ritter, J.K. Role of Nitric Oxide in the Cardiovascular and Renal Systems. *Int. J. Mol. Sci.* 19(9), 2605 (2018).
  45. Tucker, A.T., Pearson, R.M., Cooke, E.D. & Benjamin, N. Effect of nitric-oxide-generating system on microcirculatory blood flow in skin of patients with severe Raynaud's syndrome: a randomised trial. *Lancet* 354(9191), 1670-1675 (1999).
  46. Herrick, A. The pathogenesis, diagnosis and treatment of Raynaud phenomenon. *Nat. Rev. Rheumatol.* 8, 469–479 (2012).
  47. Hughes, M. & Herrick, A.L. Raynaud's phenomenon. *Best Pract. Res. Clin. Rheumatol.* 30(1), 112-132 (2016).
  48. Luo, Y., Wang, Y., Wang, Q., Xiao, R. & Lu, Q. Systemic sclerosis: genetics and epigenetics. *J. Autoimmun.* 41, 161-167 (2013).
  49. Grotewold, L. & R  ther, U. The Fused toes (Ft) Mouse Mutation Causes Anteroposterior and Dorsoventral Polydactyly. *Dev. Biol.* 251(1), 129-141 (2002).
  50. D  az-Hern  ndez, M.E., Rios-Flores, A.J., Abarca-Buis, R.E., Bustamante, M. & Chimal-Monroy, J. Molecular Control of Interdigital Cell Death and Cell Differentiation by Retinoic Acid during Digit Development. *J. Dev. Biol.* 2(2), 138-157 (2014).
  51. Hu, W., Xin, Y., Zhang, L., Hu, J., Sun, Y. & Zhao, Y. Iroquois Homeodomain transcription factors in ventricular conduction system and arrhythmia. *Int. J. Med. Sci.* 15(8), 808-815 (2018).
  52. Jung, I.H., Jung, D.E., Chung, Y.Y., Kim, K.S. & Park, S.W. Iroquois Homeobox 1 Acts as a True Tumor Suppressor in Multiple Organs by Regulating Cell Cycle Progression. *Neoplasia* 21(10), 1003-1014 (2019).
  53. K  ster, M.M., Schneider, M.A., Richter, A.M., Richtmann, S., Winter, H., Kriegsmann, M., Pullamsetti, S.S., Stiewe, T., Savai, R., Muley, T. & Dammann, R.H. Epigenetic Inactivation of the Tumor Suppressor IRX1 Occurs Frequently in Lung Adenocarcinoma and Its Silencing Is Associated with Impaired Prognosis. *Cancers (Basel)* 12(12), 3528 (2020).

54. Lee, J.Y., Lee, W.K., Park, J.Y. & Kim, D.S. Prognostic value of Iroquois homeobox 1 methylation in non-small cell lung cancers. *Genes Genomics* 42(5), 571-579 (2020).
55. Young, J., Ménétrey, J. & Goud, B. RAB6C is a retrogene that encodes a centrosomal protein involved in cell cycle progression. *J. Mol. Biol.* 397(1), 69-88 (2010).
56. Zhen, Y., Pavez, M. & Li, X. The role of Pcdh10 in neurological disease and cancer. *J. Cancer Res. Clin. Oncol.*, (2023).
57. Terkelsen, T., Pernemalm, M., Gromov, P., Børresen-Dale, A.L., Krogh, A., Haakensen, V.D., Lethiö, J., Papaleo, E. & Gromova, I. High-throughput proteomics of breast cancer interstitial fluid: identification of tumor subtype-specific serologically relevant biomarkers. *Mol. Oncol.* 15(2), 429-461 (2021).
58. Bycroft, C., Freeman, C., Petkova, D., Band, G., Elliott, L.T., Sharp, K., Motyer, A., Vukcevic, D., Delaneau, O., O'Connell, J., et al. The UK Biobank resource with deep phenotyping and genomic data. *Nature* 562, 203–209 (2018).
59. Leitsalu, L., Haller, T., Esko, T., Tammesoo, M.L., Alavere, H., Snieder, H., Perola, M., Ng, P.C., Mägi, R., Milani, L., Fischer, K. & Metspalu, A. Cohort Profile: Estonian Biobank of the Estonian Genome Center, University of Tartu. *Int. J. Epidemiol.* 44(4), 1137-1147 (2015).
60. Karlson, E., Boutin, N., Hoffnagle, A. & Allen, N. Building the Partners HealthCare Biobank at Partners Personalized Medicine: informed consent, return of research results, recruitment lessons and operational considerations. *J. Pers. Med.* 6(1), (2016).
61. Boutin, N., Holzbach, A., Mahanta, L., Aldama, J., Cerretani, X., Embree, K., Leon, I., Rathi, N. & Vickers, M. The information technology infrastructure for the translational genomics core and the partners biobank at partners personalized medicine. *J. Pers. Med.* 6(1), 1-6 (2016).
62. Boutin, N.T., Mathieu, K., Hoffnagle, A.G., Allen, N.L., Castro, V.M., Morash, M., O'Rourke, P., Hohmann, E., Herring, N., Bry, L., et al. Implementation of electronic consent at a Biobank: an opportunity for precision medicine research. *J. Pers. Med.* 6(2), 1-11 (2016).
63. Dashti, H.S., Cade, B.E., Stutaite, G., Saxena, R., Redline, S. & Karlson, E.W. Sleep Health, Diseases, and Pain Syndromes: findings from an electronic health record biobank. *Sleep* 44(3) (2020).
64. Kurki, M.I., Karjalainen, J., Palta, P., Sipilä, T.P., Kristiansson, K., Donner, K.M., Reeve, M.P., Laivuori, H., Aavikko, M., Kaunisto, M.A., et al. FinnGen provides genetic insights from a well-phenotyped isolated population. *Nature* 613(7944), 508-518 (2023).
65. Browning, B.L., Tian, X., Zhou, Y. & Browning, S.R. Fast two-stage phasing of large-scale sequence data. *Am. J. Hum. Genet.* 108(10), 1880-1890 (2021).
66. Manichaikul, A., Mychaleckyj, J.C., Rich, S.S., Daly, K., Sale, M. & Chen, W.M. Robust relationship inference in genome-wide association studies. *Bioinformatics* 26(22), 2867-2873 (2010).

67. The 1000 Genomes Project Consortium, *Nature* 526, 68-74 (2015).
68. Mbatchou, J., Barnard, L., Backman, J., Marcketta, A., Kosmicki, J.A., Ziyatdinov, A., Benner, C., O'Dushlaine, C., Barber, M., Boutkov, B., et al. Computationally efficient whole-genome regression for quantitative and binary traits. *Nat. Genet.* 53, 1097–1103 (2021).
69. Alkes, L., Price, A.L., Weale, M.E., Patterson, N., Myers, S.R., Need, A.C., Shianna, K.V., Ge, D., Rotter, J.I., Torres, E., et al. Long-Range LD Can Confound Genome Scans in Admixed Populations. *Am. J. Hum. Gen.* 83, 132-135 (2008).
70. Boughton, A.P., Welch, R.P., Flickinger, M., VandeHaar, P., Taliun, D., Abecasis, G.R. & Boehnke, M. LocusZoom.js: interactive and embeddable visualization of genetic association study results. *Bioinformatics* 37(18), 3017-3018 (2021).
71. GTEx Consortium. The GTEx Consortium atlas of genetic regulatory effects across human tissues. *Science* 369(6509), 1318-1330 (2020).
72. Wang, G., Sarkar, A., Carbonetto, P., Stephens, M. A Simple New Approach to Variable Selection in Regression, with Application to Genetic Fine Mapping. *Journal of the Royal Statistical Society Series B: Statistical Methodology*, Volume 82, Issue 5, December 2020, Pages 1273–1300.
73. Wallace, C. A more accurate method for colocalisation analysis allowing for multiple causal variants. *PLoS Genet.* 17(9), (2021).
74. Liu, B., Gludemans, M.J., Rao, A.S., Ingelsson, E. & Montgomery, S.B. Abundant associations with gene expression complicate GWAS follow-up. *Nat. Genet.* 51(5), 768-769 (2019).
75. Zhao, Q., Dacre, M., Nguyen, T., Pjanic, M., Liu, B., Iyer, D., Cheng, P., Wirka, R., Kim, J.B., Fraser, H.B. & Quertermous, T. Molecular mechanisms of coronary disease revealed using quantitative trait loci for TCF21 binding, chromatin accessibility, and chromosomal looping. *Genome Biol.* 21(1), 135 (2020).